Electronic Supplementary Material (ESI) for Lab on a Chip.

Peristaltic on-chip pump for tunable media circulation and whole blood perfusion in PDMS-free organ-on-chip and organ-disc systems

Authors

Stefan Schneider[a], Marvin Bubeck[a,b], Julia Rogal[a,c], Huub J. Weener[a,d], Cristhian Rojas[e], Martin Weiss[e,f], Michael Heymann[b], Andries D. van der Meer[d] and Peter Loskill[a,c,e,g,*]

[a] Fraunhofer Institute for Interfacial Engineering and Biotechnology IGB, Stuttgart, Germany
[b] Institute of Biomaterials and Biomolecular Systems, University of Stuttgart, Stuttgart, Germany
[c] Department of Biomedical Engineering, Faculty of Medicine, Eberhard Karls University Tübingen, Tübingen, Germany
[d] Applied Stem Cell Technologies, University of Twente, Enschede, The Netherlands
[e] NMI Natural and Medical Sciences Institute at the University of Tübingen, Reutlingen, Germany
[f] Department of Women's Health, Faculty of Medicine, Eberhard Karls University Tübingen, Tübingen, Germany
[g] 3R-Center for *in vitro* Models and Alternatives to Animal Testing, Eberhard Karls University Tübingen, Tübingen, Germany
* Corresponding author: peter.loskill@uni-tuebingen.de

Supplementary information

Channel layout, dimensions and hydraulic properties

Three main iterations of the pump channel design were performed during preliminary tests: i) pump channel width was varied between 400-1000 µm while keeping a constant steel ball diameter of 5 mm. Pump tests revealed that all dimensions were suitable for pushing liquid through the system. The pumped flow rate but also the fluctuation of the respective flow rate increased with wider pump channels. ii) We added a TPE pump support layer underneath the pump channels in order to press the pump channel cover in to a soft material instead of the hard surface of the PMMA disc. iii) We used rounded pump channel corners with an outer radius of 600 µm instead of rectangular corners in order to achieve a smoother, gradual entrance and exit of the steel ball in and out of the pump channel.

The final channel layout of the peristaltic Organ-Disc is presented as top view of both PMMA and TPE module featuring in total four individual systems (Supplementary figure 1). Each system features a cell, connector and pump channel (cf. Supplementary table 1 for the individual channel dimensions).

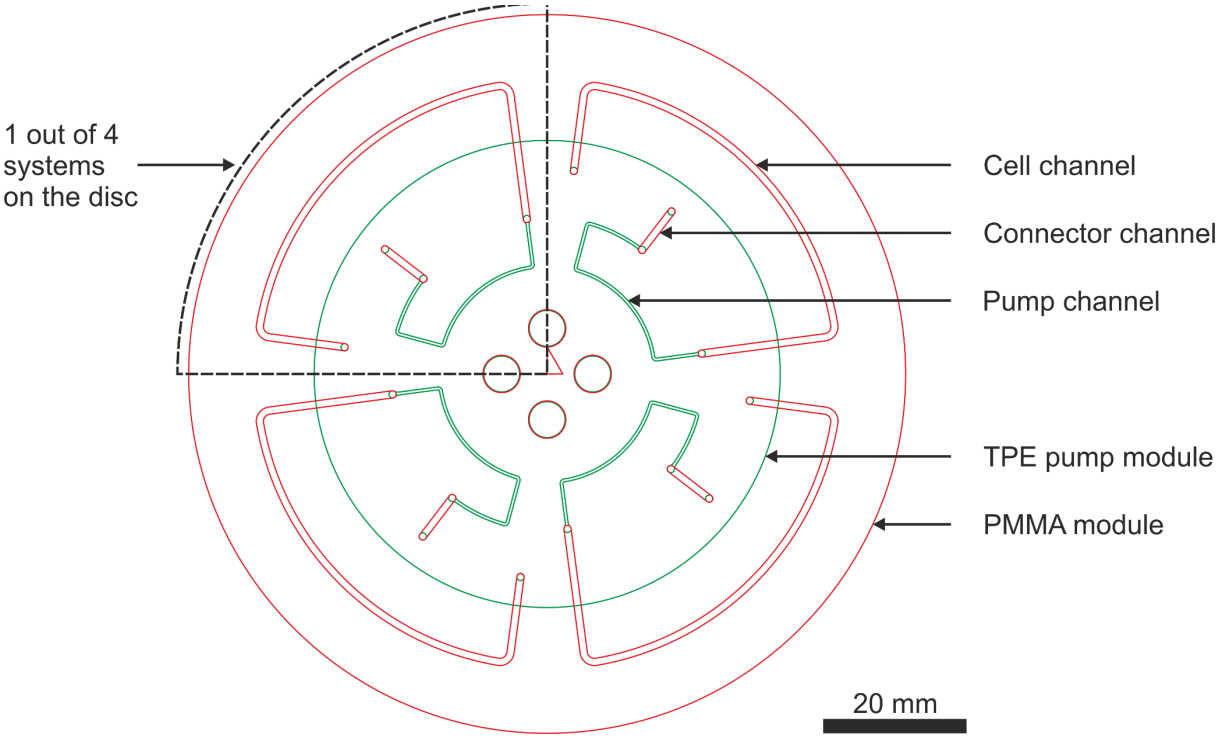

Supplementary figure 1: Channel layout of the peristaltic Organ-Disc with four individual systems per disc.

The hydraulic resistance R_{hyd} is calculated for the individual, rectangular channels of the disc with

$$R_{\mathrm{hyd}} = \frac{12\eta L}{\left[1 - 0.63\left(\frac{H}{W}\right)\right] H^3 W},$$

which provides a good estimation for channels with a H / W < 1.[1] In our case H /W = 0.18 for cell and connector channel and H / W = 0.24 for the pump channel. The hydraulic resistance of the complete channel is the sum of the individual resistances of the in-line connected channels (Supplementary table 1).

Supplementary table 1: Channel height H, width W from channel cross sections and channel length L as well as volume V from CAD design. Total system volume calculated as sum of all channel volumes and the reservoir ports (diameter 1 mm, height 2 mm). Hydraulic resistance of the individual, in-line connected channel segments and the total hydraulic resistance of a disc system. (η = 1 mPa s)

	H [µm]	W [µm]	L (CAD) [mm]	V (CAD) [µL]	R_{hyd} [Pa · s / m³]
Cell channel	170 ± 15	963 ± 28	83.9	15	2.4×10^{11}
Connector channel	170 ± 15	963 ± 28	7.7	2	2.2×10^{10}
Pump channel	96 ± 1	406 ± 5	38.2	4	1.5×10^{12}
System				∑ = 24	∑ = 1.8×10^{12}

The pressure drop Δ*p* of a system on the disc is estimated using

$$\Delta p = R_{\mathrm{hyd}} \cdot Q$$

for each measured flow rate (Supplementary table 2). The respective Reynolds number Re in the cell channel at each flow rate is calculated using

$$Re = \frac{D_{\mathrm{h}} \bar{v} \rho}{\eta}$$

with the hydraulic equivalent diameter of the cell channel

$$D_{\mathrm{h}} = 4 \frac{H \cdot W}{H + W}$$

and the average flow velocity

$$\bar{v} = \frac{Q}{H \cdot W}.$$

Supplementary table 2: Pressure drop Δp of a system on the disc and the Reynolds number Re in a cell channel for the individual, measured flow rates.

U_{Motor} [rph]	Q [mL / h]	Δ*p* [Pa]	$Re_{\mathrm{cell\ channel}}$ [-]
100	0.32	156	0.31
200	0.64	314	0.63
400	1.3	628	1.3
800	2.6	1252	2.5

Channel cross sections

Intact cross sections of TPE pump channels and PMMA cell channels after microstructuring and bonding demonstrate the precise microfabrication processes used for Organ-Disc fabrication (Supplementary figure 2).

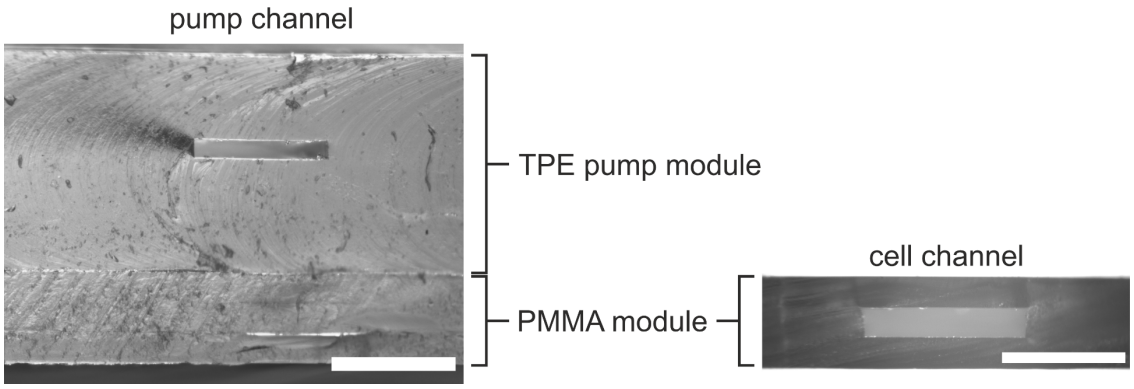

Supplementary figure 2: Cross section of a TPE pump module (preliminary pump channel design with 800 µm channel width) and a PMMA cell channel after bonding. Scale bars: 750 µm.

Theoretical flow rate

The number of steel balls above the pump channels is such that at least one steel ball is constantly acting and hence sealing the pump channel (Supplementary figure 3 a). Before a steel ball leaves the pump channel, the next one in line is already compressing the channel. Between two neighboring steel balls, a constant volume of media is trapped and pushed through the channel. This volume V_{theo} can be estimated as

$$V_{theo} = \frac{\pi D_m A_{cs}}{n} - \alpha \,,$$

with D_m = 30 mm the diameter of the circular trajectory of the steel balls rolling over the disc, A_{cs} = 100 µm × 400 µm the cross sectional area of the pump channel, n = 8 the number of steel balls and α taking into account the displacement of the steel balls compressing the pump channel (Supplementary figure 3 b). The theoretical flow rate Q_{theo} is then

$$Q_{theo} = UnV_{theo} \,,$$

with U the number of motor revolutions per time.

In the simplest case of α = 0, V_{theo} is the inner pump channel volume between the center of two steel balls. Thereby, the deflection of the pump channel ceiling is ignored, which reduces the trapped media volume between the steel balls. Already for the simplest case of α = 0, Q_{theo} is in good agreement with the experimental measurements (Supplementary figure 3 c). However, α = 0, leads to an overestimation and, thus the measured flow rates are shifted to

slightly lower values, because channel compression by the steel balls reduces the transported fluid volume. The difference between experimental flow rates and theoretical flow rates for $\alpha = 0$ reveals the actual compression and reduction of the trapped volume. In average, the compression of both steel balls is $\alpha = 0.071$ µL.

The compression α allows for an estimation of the fluid volume that can flow back due to peristalsis every time a steel ball leaves the pump channel or a new steel ball enters the pump channel (Supplementary figure 4). The deflection of a single steel ball is $\alpha / 2 = 0.036$ µL. In theory, this volume can flow back from the cell channel into the pump channel once a steel ball leaves the pump channel (Supplementary figure 4; phase 1 and phase 2). In the case of a steel ball entering the pump channel, this volume is pushed back into the reservoir (Supplementary figure 4; phase 3 and phase 4).

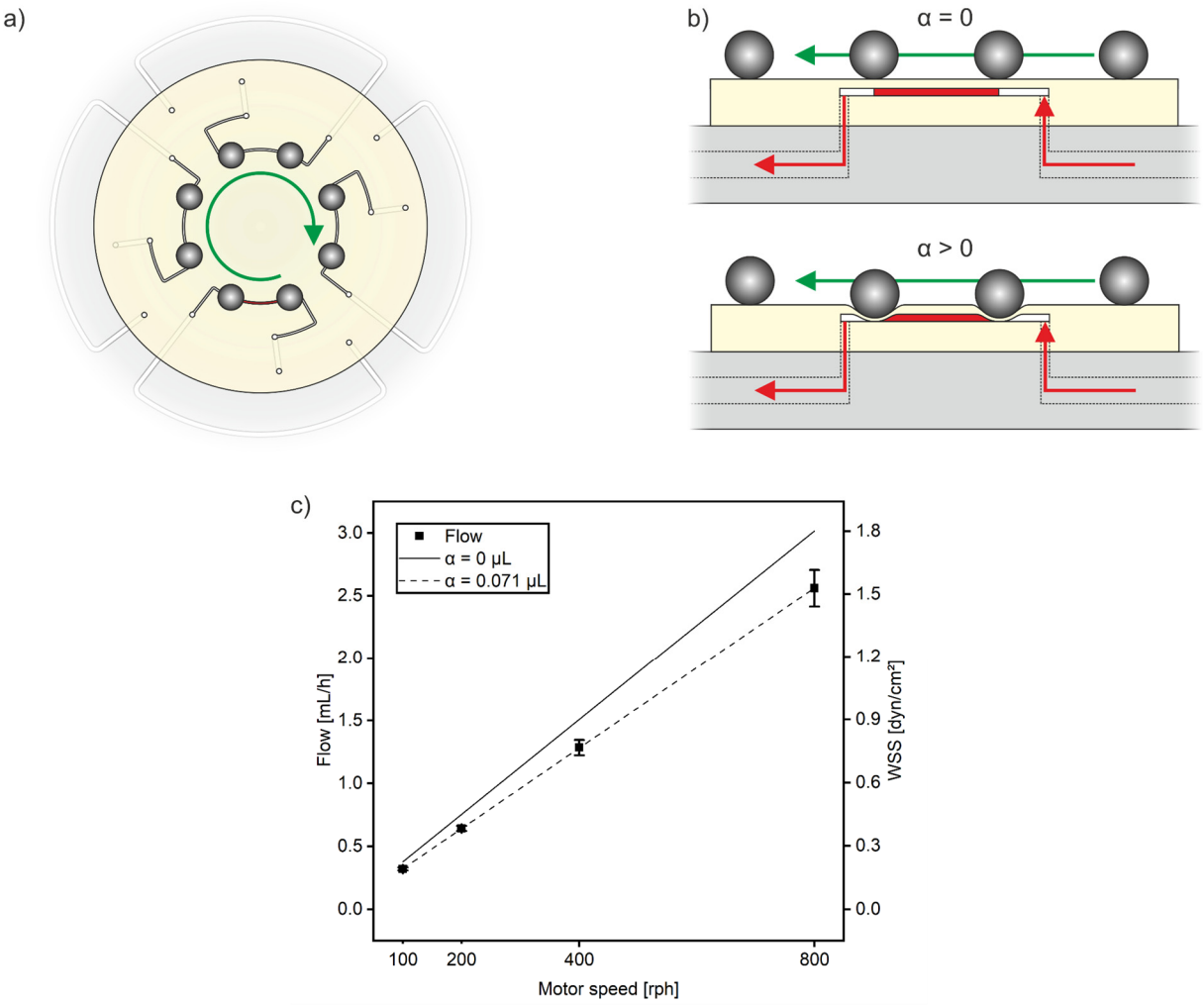

Supplementary figure 3: Theoretical flow rate of the integrated, peristaltic pump. a) Top view of the disc: A constant volume (red) is pushed through the system each time a pair of steel balls rolls over the pump channel. b) Side view of a pump channel: In the simplest case, the constant, transported volume (red) can be estimated as the whole, inner channel volume between two steel balls. If the deflection of the steel balls and the flexible TPE top layer is considered, this transported volume will be further reduced. (not drawn to scale) c) Measured and theoretical flow rates for the case of no steel ball compression (α = 0 µL) and the calculated compression derived from measured rates (α = 0.071 µL). Flow rates of two tested, independent systems, each measured three time.

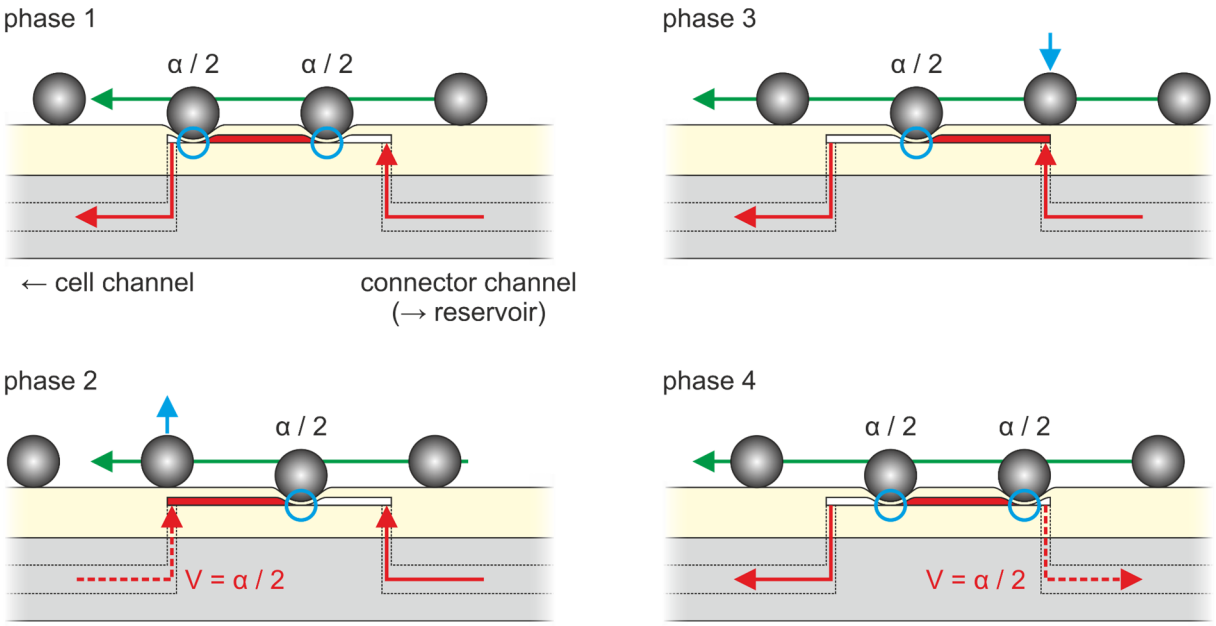

Supplementary figure 4: Peristalsis of the pump. If a steel ball leaves the pump channel the displaced volume of a steel ball (α / 2) can flow back into the pump channel (phase 1 and 2). If another steel ball enters the pump channel, the displaced volume is pushed into the reservoir (phase 3 and 4).

Back pressure influence on flow rate

For flow rate measurements, a simple setup of two syringes attached to the in- and outlet of a system was used. Both syringes were filled with equal amounts of dyed water and volume displacement monitored over time. The water height difference between both syringes and a corresponding hydrostatic pressure difference increase over time (Supplementary figure 5 a). Flow rates at varying motor speed did, however, not decrease with increasing back pressure (Supplementary figure 5 b). Up to the maximum applied back pressure of approx. 450 Pa, resulting from the maximum height difference in the syringes during measurements, no decrease in flow rate was observable. This indicates that the steel balls compressing the pump channel allow for a tight sealing that prevents back flow.

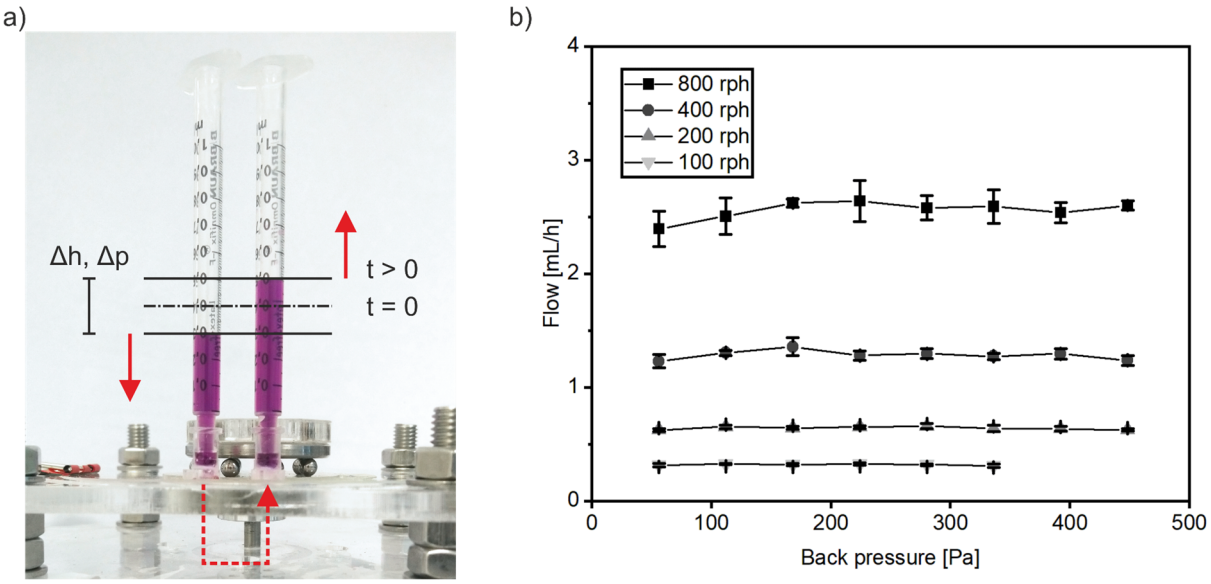

Supplementary figure 5: Back pressure influence on flow rate. a) Photograph of the flow measurement setup: Two syringes are attached to the in- and outlet of a system, filled with colored water and volume changes during peristaltic pumping are monitored over time. This allows for a simple assessment of the flow rate and at the same time for an evaluation of the back pressure influence due to height differences in water level in both syringes. b) Flow rates for varying motor speeds: With increasing back pressure over measurement time, no decrease in flow rate is observable up to the maximum back pressure built up during measurements (approx. 450 Pa). This indicates that compressed pump channels are sealed and no back flow occurs. Flow rates of two tested, independent systems, each measured three times.

Flow stability

Flow rate measurements were conducted within a period of three days. In order to show the stability of the peristaltic pump and to allow for a comparison between different pump settings, the measured flow rates were normalized to the motor revolutions per time. Both tested systems pumped comparable fluid volumes for each motor speed and on each day close to the average over all measurements (Supplementary figure 6).

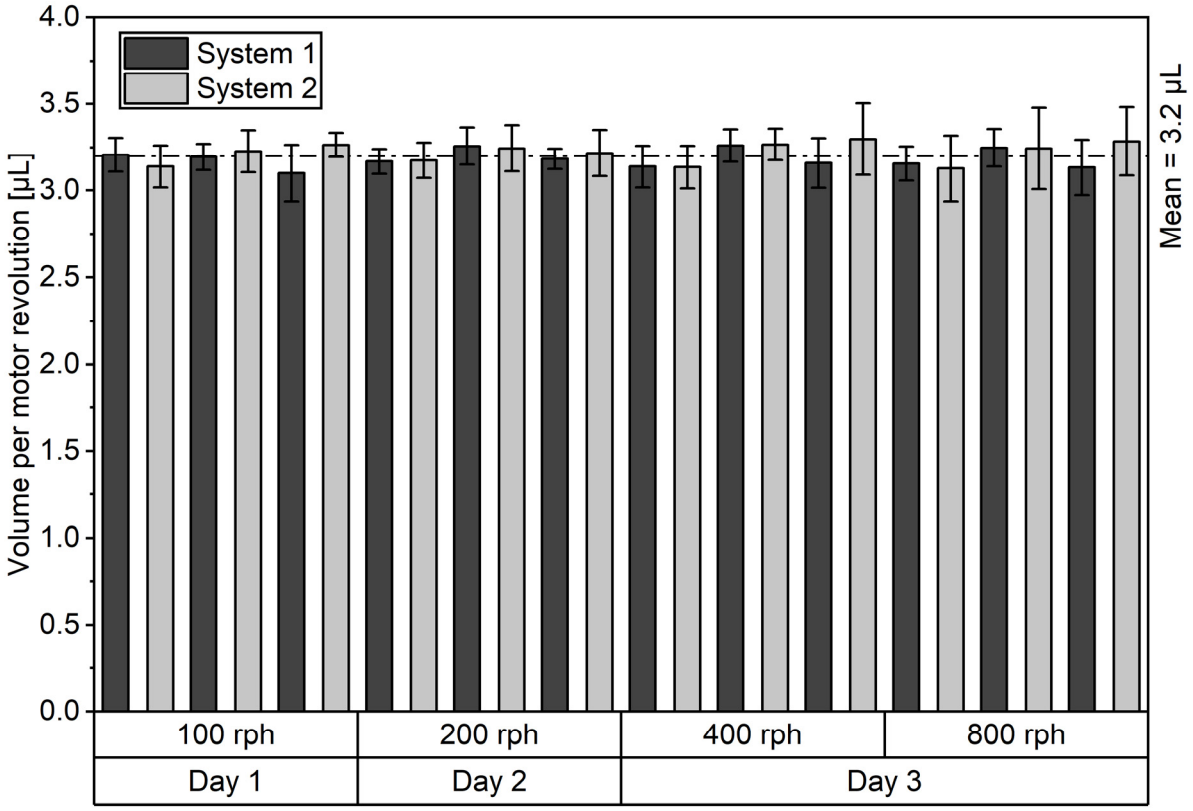

Supplementary figure 6: Flow stability of the peristaltic pump. Volume per motor revolution of flow rate measurements over three days.

Calculation of the total media volume from ion concentrations

The total amount $N_t(i)$ of each ion *i* inside the perfused reference system without cells is balanced each day *t* using

$$N_t(i) = N_{t-1}(i) + V_P[c_0(i) - c_{t-1}(i)]$$

and considering the replacement of drawn sample volume V_P by equal amounts of fresh cell culture media with a concentration c_0 of each component *i*. Every three days, following sampling and analysis, the supernatant inside the reservoir compartment was aspirated and replaced with the initial starting volume V_0 = 5 mL of fresh cell culture media. The system was not flushed during media exchange to prevent unintentional cell detachment from uncontrolled manual flushing, hence, the inner volume of a system V_S (approx. 24 µL) will still contain old media after the reservoir compartment is refilled with fresh cell culture media. Therefore, the total amount of each solute is

$$N_{t\,=\,exchanged}(i) = V_0 c_0(i) + V_S c_S(i)$$

after each media exchange (*t* = *exchanged*). Assuming that within 24 h of perfusion - thereby at each time point of sampling *t* - the complete media volume in channel and compartment is homogenously mixed,

$$c_t(i) = c_S(i)\,,$$

the analyzed sample then represents the complete media volume inside reservoir and inner channel volume. As media exchange and sampling are the only processes affecting the number of ions, the remaining, total volume V_t can be calculated as

$$V_t = \frac{N_t(i)}{c_t(i)}\,.$$

Estimation of oxygen consumption

The oxygen consumption rate of HUVECs is estimated using previously reported basal mitochondrial respiration of approx. 80 × 10^{-12} mol/min of in total 30,000 cells.[2] This results in an oxygen consumption per cell of approx. *OC* = 2.7 × 10^{-15} mol/min/cell.

The cell amount inside the cell channel of the Organ-Disc is estimated from counts of Hoechst stained nuclei on a confluent cell channel section (rectangular ROI size 635.98 × 663.38 µm^2) using Fiji's Analyze Particle function (Image J version 1.53c).[3] This results in 455 cells / ROI and approx. *n* = 180,000 cells in total on top and bottom of the cell channel with a total surface of approx. 167 mm^2.

For this estimation, we assume cell culture media flowing into the cell channel to be saturated with an oxygen concentration of c_{in} = 192 × 10^{-6} mol/L.[4] We balance oxygen input with the oxygen consumption of the cells inside the cell channel at a flow rate *Q* with

$$c_{out} = c_{in} - \frac{OC \cdot n}{Q}$$

and assuming steady state conditions. Thereby, media leaving the cell channel is saturated with 53%-94% at flow rates of 0.32-2.6 mL/h respectively (Supplementary table 3).

Supplementary table 3: Estimation of oxygen consumption of HUVECs inside the disc under different flow conditions.

Motor speed [rpm]	Q [mL/h]	c_{out} [mmol/L]	O_2 saturation [%]
100	0.32	0.10	53
200	0.64	0.15	77
400	1.3	0.17	88
800	2.6	0.18	94

References

1 H. Bruus, *Theoretical microfluidics*, Oxford University Press, Oxford ; New York, 2008.

2 E. Balogh, D. J. Veale, T. McGarry, C. Orr, Z. Szekanecz, C.-T. Ng, U. Fearon and M. Biniecka, *Arthritis Res Ther*, 2018, **20**, 95.

3 J. Schindelin, I. Arganda-Carreras, E. Frise, V. Kaynig, M. Longair, T. Pietzsch, S. Preibisch, C. Rueden, S. Saalfeld, B. Schmid, J.-Y. Tinevez, D. J. White, V. Hartenstein, K. Eliceiri, P. Tomancak and A. Cardona, *Nat Methods*, 2012, **9**, 676–682.

4 B. A. Wagner, S. Venkataraman and G. R. Buettner, *Free Radical Biology and Medicine*, 2011, **51**, 700–712.